The Möbius phenomenon in Generalized Möbius-Listing surfaces and bodies, and Arnold's Cat phenomenon

The Möbius phenomenon in Generalized Möbius-Listing surfaces and bodies, and Arnold's Cat phenomenon

Johan Gielis[1,*], Paolo Emilio Ricci[2], Ilia Tavkhelidze[3]

1 University of Antwerp, Department of Biosciences Engineering, Belgium
2 UniNettuno International Telematic University, 00186 Rome, Italy
3. Tbilisi State University, Faculty of Exact and Natural Sciences, Tbilisi 0186, Georgia.
* Correspondence: johan.gielis@uantwerpen.be

Abstract: Möbius bands have been studied extensively, mainly in topology. Generalized Möbius-Listing surfaces and bodies providing a full geometrical generalization, is a quite new field, motivated originally by solutions of boundary value problems. Analogous to cutting of the original Möbius band, for this class of surfaces and bodies, results have been obtained when cutting such bodies or surfaces. In general, cutting leads to interlinked and intertwined different surfaces or bodies, resulting in very complex systems. However, under certain conditions, the result of cutting can be a single surface or body, which reduces complexity considerably. Our research is motivated by this reduction of complexity. In the study of cutting Generalized Möbius-Listing bodies with polygons as cross section, the conditions under which a single body results, displaying the Möbius phenomenon of a one-sided body, have been determined for even and odd polygons. These conditions are based on congruence and rotational symmetry of the resulting cross sections after cutting, and on the knife cutting the origin. The Möbius phenomenon is important, since the process of cutting (or separation of zones in a *GML* body in general) then results in a single body, not in different, intertwined domains.

In all previous works it was assumed that the cross section of the GML bodies is constant, but the main result of this paper is that it is sufficient that only one cross section on the whole *GML* structure meets the conditions for the Möbius phenomenon to occur. Several examples are given to illustrate this.

Keywords: Generalized Möbius-Listing Bodies and Surfaces, Möbius phenomenon, regular polygons, Gielis Transformations, Poincaré Recurrence Theorem.

1. Introduction

Generalized Möbius-Listing bodies and surfaces

The Möbius band, a ribbon with a twist (Figure 1a), is an icon of mathematics. It is well known that cutting a Möbius band along the basic line or parallel to the basic line, yields either a single (Link-1) or two connected bodies (Link-2) for Möbius bands. The general case of cutting Möbius bands or ribbons with any number of twists, odd and even (Figure 1b,c,d), and any number of knives ,was solved in *[1].*

Möbius bands have been studied mainly in topology because of the phenomenon of non-orientability and one-sidedness, but also from a geometrical point of view, see e.g. *[2]*. Only recently Generalized Möbius-Listing GML_m^n surfaces and bodies have been introduced *[3,4]*. These are toroidal structures obtained from prisms with cross section with rotational symmetry m and with the centers of all cross sections forming the basic line of the toroidal structure (Fig 2). Without loss of generality, the cross sections can be regular polygons P_m (with the circle P_∞ yielding the classical torus). If the cross section is a line, one can obtain an annulus, or any shapes as shown in Figure 1.

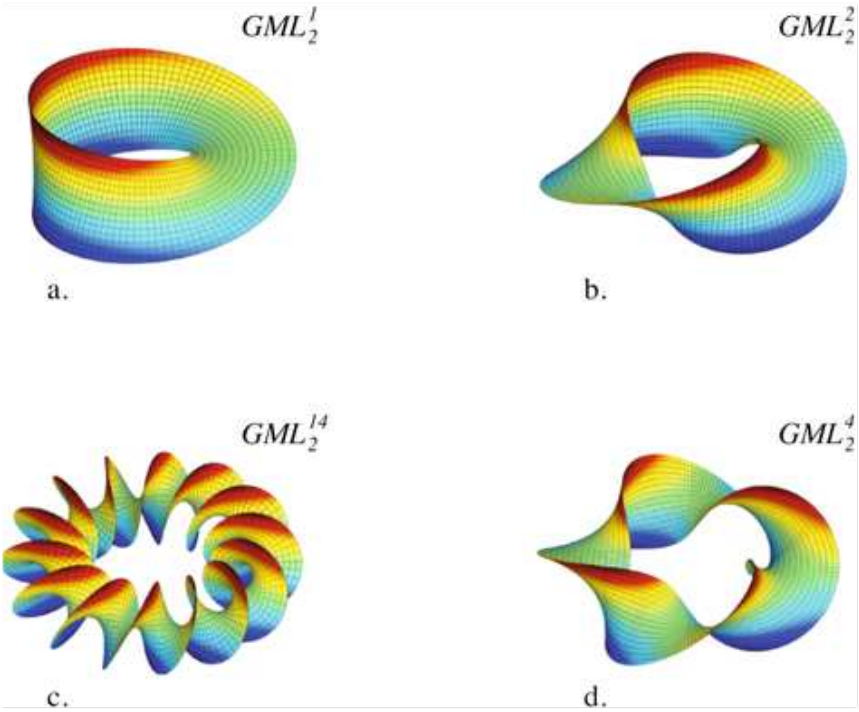

Figure 1: Ribbons with n twists of 180°. GML_2^1 (a) is the Möbius band

The following definitions are needed *[5]*:

Definition 1: The toroidal structure of GML_m^n surfaces and bodies, results from joining the two ends of the cylinder after n twists of the prism around the basic line, with both m and n positive integers.

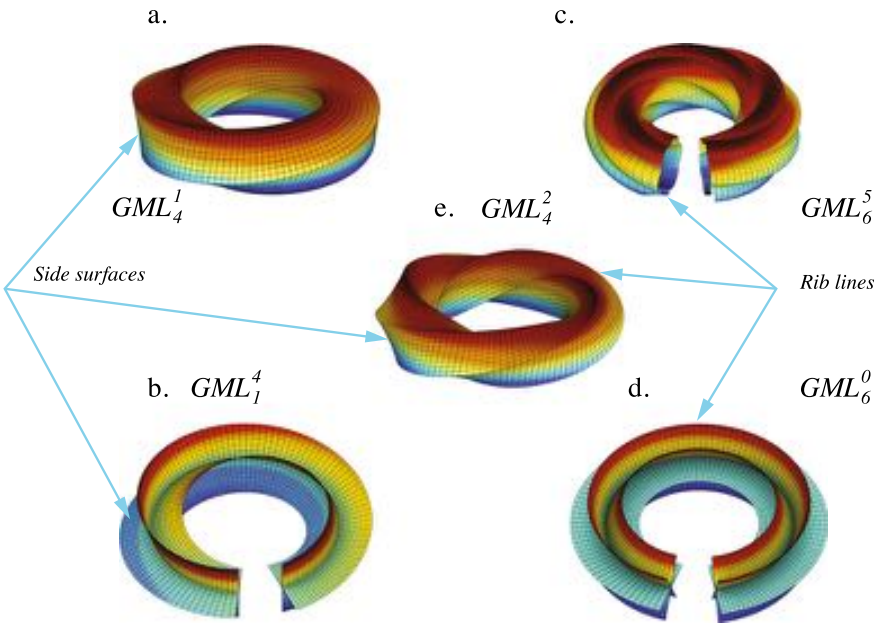

Figure 2: (a-e) Identification of vertices, with twists leading to torus GML_m^n.

Generalized Möbius-Listing Bodies GML_m^n are defined analytically by (1) and (2):

$$\begin{cases} X(\tau,\psi,\theta,t) = T_1(t) + \left[R(\psi,\theta,t) + p(\tau,\psi,\theta,t)\cos(\frac{n\theta}{m}) - q(\tau,\psi,\theta,t)\sin\left(\frac{n\theta}{m}\right)\right]\cos(\theta + M(t)) \\ Y(\tau,\psi,\theta,t) = T_2(t) + \left[R(\psi,\theta,t) + p(\tau,\psi,\theta,t)\cos(\frac{n\theta}{m}) - q(\tau,\psi,\theta,t)\sin\left(\frac{n\theta}{m}\right)\right]\sin(\theta + M(t)) \\ Z(\tau,\psi,\theta,t) = T_3(t) + Q(\theta,t) + \left[p(\tau,\psi,\theta,t)\sin\left(\frac{n\theta}{m}\right) + q(\tau,\psi,\theta,t)\cos(\frac{n\theta}{m})\right] \end{cases} \quad (1)$$

or, alternatively,

$$\begin{cases} X(\tau,\psi,\theta,t) = T_1(t) + \left[R(\theta,t) + p(\tau,\psi,\theta,t)\cos(\psi + \frac{n\theta}{m})\right]\cos(\theta + M(t)) \\ Y(\tau,\psi,\theta,t) = T_2(t) + \left[R(\theta,t) + p(\tau,\psi,\theta,t)\cos(\psi + \frac{n\theta}{m})\right]\sin(\theta + M(t)) \\ Z(\tau,\psi,\theta,t) = T_3(t) + Q(\theta,t) + p(\tau,\psi,\theta,t)\sin\left(\psi + \frac{n\theta}{m}\right) \end{cases} \quad (2)$$

X, Y, Z, t is the ordinary notation for space and time coordinates and τ, ψ, θ are local coordinates where $\tau \in [-\tau^*, \tau^*]$, with $0 < \tau$; $\psi \in [0; 2\pi]$ and $\vartheta \in [0; 2\pi h]$, with $h \in \mathbb{R}$. The functions $T_{1,2,3}(t), R(\psi,\theta,t), p(\tau,\psi,\theta,t), M(t)$ and $Q(\theta,t)$, as well as parameter $\mu = \frac{n}{m}$, define simple movements. With these analytic representations, complex movements can be studied and decomposed into simple ones *[6]*, allowing the study of this class of surfaces and bodies from a kinematic point of view. However, the same parameterizations also lend themselves to dynamic studies, with, for example, changing cross sections in time.

Definition 2: The basic line of a GML_m^n body is the continuous closed, generally spatial curve, generated by the center of the prism in its movement necessary to obtain, after n twists, the joining of the two opposite faces of the prism.

This basic line can be a circle P_∞ (and any curve homeomorphic to a circle) or a self-intersecting curve like a Pascal's limaçon (Figure 3a). This is a self-intersecting figure closing after two full rotations. The basic line can also be other planar or space curves, for example, a rose curve $\rho = \cos m\theta$. In this general case the notation $GML_m^n(v)$ is used with $v \in \mathbb{Q}$ denoting the shape of the basic line, with $v = 1$ if the basic line is a circle.

Definition 3. The **twisting parameter** $\mu = \frac{n}{m}$ describes the characteristic of twisting where m is the number of vertices of the regular polygon P_m (the shape of the radial cross section) and n is the number of twisting of the cross section of the prism before identification of its ends. If $\mu = \frac{n}{m}$ is an integer number $(n = km)$, then the corresponding lines makes k coils after one rotation around the torus. If $\frac{n}{m} \in \mathbb{Q}$ then the corresponding line makes n coils after m rotations around the torus. If $\frac{n}{m} \in \mathbb{R} \setminus \mathbb{Q}$ then the line makes infinite coils after infinite rotations around the torus without self-intersections.

Definition 4: A **rib** of the $GML_m^n(v)$ for each $v \in \mathbb{Q}$, is a continuous closed, in the general case, spatial line on which are situated only the vertices of the radial cross section of this body (i.e., the torus line with characteristic $\frac{n}{m}$).

Between the ribs, planes or curved surfaces can be spanned giving rise to a GML_m^n side surfaces (Figure 2), and if the whole structure is solid (i.e., all cross sections are disks), then one obtains GML_m^n bodies. Obviously one can also define shell structures, by limiting the radial function of the cross sections.

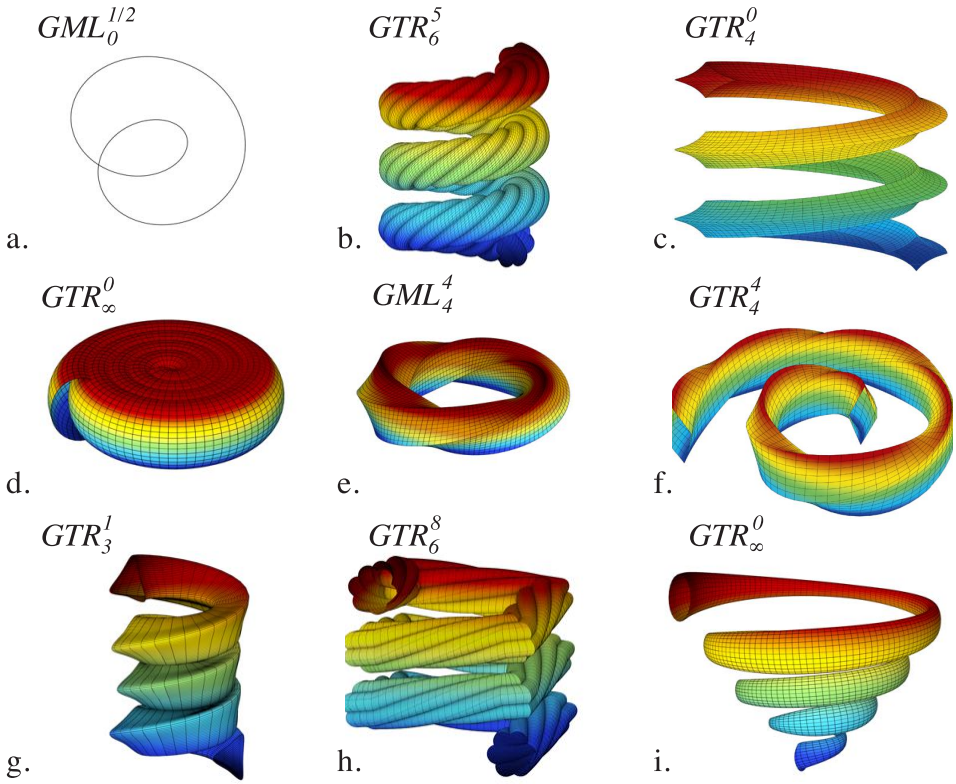

Figure 3: **a.** $GML_0^{1/2}$ **b-i:** Examples of GTR_m^n surfaces with and without torsion. **e**. closed GML_4^4

GML_m^n bodies and surfaces are always closed. They are a subset of closed Generalized Twisting and Rotating bodies GTR_m^n. In this general, case the ends of the prims need not be closed and the basic line can be a spiral (Figure 3f) or a helix (Figure 3b,c).

The original motivation to study GML_m^n surfaces and bodies is that the solution of boundary value problems for partial differential equations is easier to obtain with direct knowledge of the domain and, with the extension of surfaces to bodies, also of the internal geometry and connected domains inside GML_m^nbodies. It allows to understand the precise relation between the asymptotic behavior of solutions and the geometrical structure of boundary. A number of studies have focused on elasticity of Möbius bands only *[2, 7]*, but the general problem is open.

As a generalization of Möbius bands, cutting of GML_m^n surfaces and bodies has also been studied. We will discuss this in Section 2 and show that the problem of cutting (Definition 5) is reduced to a problem of planar geometry, whereby the results depend only the cross section $p(\tau, \psi, t)$ and the twisting parameter n.

Definition 5: Cutting of a GML_m^n body with a regular polygon as cross section is performed with (1) a straight knife, which (2) cuts perpendicular to the polygonal cross section of the surfaces and bodies, and (3) the knife cuts the m-polygon boundary exactly in two points or two times (depending on the thickness of the knife). For (3) there are three possibilities: the cut of the polygon can be from a vertex to a vertex VV, from a vertex to a side or edge VS, or from side to side SS (=edge to edge). The precise orientation of this knife (and the positions where it cuts the boundary) is maintained during the complete cutting process, until the knife returns to its starting position, and the cutting is completed.

The point of the knife traces out a toroidal line along the body or surface. In general, cutting leads to separate bodies or surfaces, but in particular cases a single body results, similar to the single surface that results from cutting the original Möbius band along the basic line. In analogy with the cutting of a classic Möbius band along the central line, we define the Möbius phenomenon as follows:

Definition 6: The Möbius phenomenon occurs when, after cutting of a GML_m^n body or surface, a single body or surface results, where one can travel along a rib or a side surface and return to the original position. We say that the Mobius phenomenon appears if moving continuously along a rib or a side surface, it is possible to return at the initial position.

Given that the cutting of GML_m^n surfaces and bodies in general gives rise to very complex structures of intertwined different surfaces and bodies, our main motivation is the search for the conditions that result in a single GML_m^n surface or body after cutting, thereby greatly reducing complexity.

A model for natural phenomena

In various fields of science Möbius ribbons or topologies are observed, from chemistry to physics, and increasingly so *[8-12]*. It should not be very surprising then that GML_m^n surfaces and bodies will find application in science; models of mollusk shells and tornados *[6]*, circular DNA or the helical heart *[13]*, are straightforward examples. Mollusk shells and tornados are examples of non-closed structures (GTR_m^n), whereas circular DNA (with a circle as basic line) and the helical heart (*[13]* with a limaçon as basic line) are examples of GML_m^n structures.

They can also be models for more complex phenomena, but then, first and foremost, it is necessary to understand the geometry of GML_m^n bodies to be able to observe these phenomena. Figure 4a shows a GML_5^n body in blue. The other panels show the same body represented by point clouds, with increasing noise, which can be representative of real physical phenomena, with measurement uncertainty.

It will depend on the accuracy of the measurement whether or not such structures can be observed. With decreasing measurement precision and no knowledge about GML_m^n structures, one might easily mistake data points resulting from measurements as toroidal (Figure 4d), or a having some structure (Figure 4b,c). This "measurement" problem will be even worse if one has only datapoints from 2D- cross sections. The structure in the Figure 4b may be interpreted as resulting from phenomena with a non-linear resonances footprint *[14]*, whereas the system is completely deterministic with a homogeneous material.

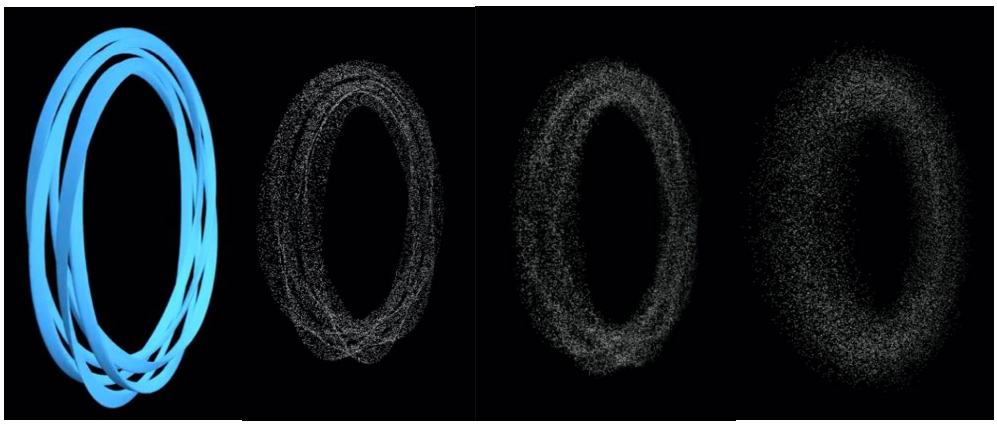

a **b** **c** **d**

Figure 4: a. GML_5^n body. B-d. The same body represented by point clouds, with increasing noise

Cutting of GML bodies and the Flatland experience

Cutting of GML bodies and surfaces

The problem gets considerably more complex if one considers that the blue structure in Figure 3 is only one of the four structures resulting from cutting the GML_5^n body (Figure 5a). Indeed, if the cross section of the GML_5^n body is cut with a knife from side 1 to side 3, and this cut is carried out along the whole GML_5^n, then four different bodies will result, identified by different colours in Figure 5a. Actually, this is a Link-4 structure with all four bodies intertwined *[15]*. An example of complex intertwined structures resulting from cutting is shown in Figure 5b.

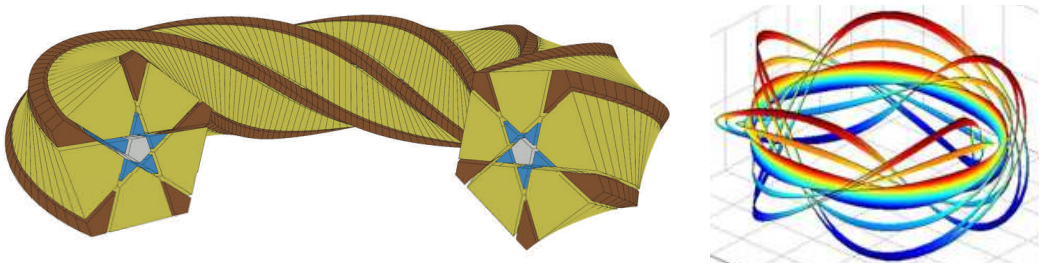

a **b**

Figure 5: a. GML_5^n body cut into four pieces, b. Structures after cutting GML_5^n surface

The process of cutting does not necessarily result in separate bodies; the lines in the cross sections in Figure 5a, may simply be lines demarcating zones with different vector or tensor fields or different scalar values. The number of such zones or independent structures depends on the type of cut [15- 17] with a knife that cuts through the cross section (from vertex i to vertex j denoted by $VV_{i,j}$; from vertex i to side j denoted by $VS_{i,j}$, or from side i to side j denoted by $SS_{i,j}$), and on the number of twists, the upper index n. In Figure 5a the cut is $SS_{1,3}$ and results in two bodies with triangular, one body with six-sided and a central one with a regular pentagon cross section, a total of four as seen in Figure 6, case B.III. Case B.IV is a similar possibility, but with one triangular, one quadrangular and two pentagonal shapes. In general, if the number of twists of GML_5^n body is $n = 5 \cdot \omega + q$, with ω=0,1,2,… and q = 1,2,3,4, then twelve possible cases appear, as displayed in Figure 6 (A to G with subcases) [15]. Furthermore, also the twisting characteristics of each of those bodies after cutting are known (Figure 6, green column Structure of elements) [15]. Hence, despite the apparent complexity, the Link-4 structure is simple and fully deterministic.

Figure 7 displays two other ways to connect the two ends of the prism to obtain a full or partial GML_4^n structure cut [16]. The structures in Figure 7a can be either a complete GML_4^n, or a partial one, with the GML_4^n continuing below the plane. Figure 7b can also be connected to a real-life phenomenon: the twisted GML_4^n with square cross section is similar to culms of square bamboos [17]. In this case the cross section is a superellipse instead of a square, and the twist is given by a deformation parameter; in other words, the cross section $p(\tau, \psi)$ is a superellipse and the deformation is given by twisting parameter n [17]. Superellipses also accurately model annual tree rings in softwood, and such trees also grow with twist and torsion [18].

AI.	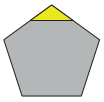	$SS_{1,2}$ $b_2^1 + b_2^2 < A$		$GML_3^{15\omega+3q+12}$ {ω + 0.2q} $GML_{10}^{10\omega+2q}$	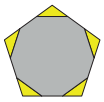	link-2
AII.	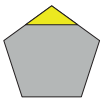	$SS_{1,2}$ $b_2^1 + b_2^2 = A$		$GML_3^{15\omega+3q+12}$ {ω + 0.2q} $GML_5^{5\omega+q}$	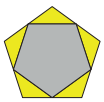	link-2
AIII.	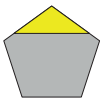	$SS_{1,2}$ $b_2^1 + b_2^2 > A$	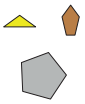	$GML_3^{15\omega+3q+12}$ {ω + 0.2q} $GML_5^{25\omega+5q+20}$ {ω + 0.2q} $GML_5^{5\omega+q}$		link-3
BI.		$SS_{1,3}$ $b_3^1 + b_3^2 < A$ b_3^1 or $b_3^2 < 0.5A$	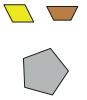	$GML_4^{20\omega+4q+16}$ {ω + 0.2q} $GML_4^{20\omega+4q+16}$ {ω + 0.2q} $GML_5^{5\omega+j}$		link-3
BII.		$SS_{1,3}$ $b_3^1 + b_3^2 = A$	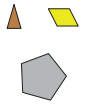	$GML_3^{15\omega+3q+12}$ {ω + 0.2q} $GML_4^{20\omega+4q+16}$ {ω + 0.2q} $GML_5^{25\omega+j}$		link-3
BIII.		$SS_{1,3}$ $b_3^1 + b_3^2 > A$ b_3^1 or $b_3^2 < 0.5A$	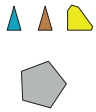	$GML_3^{15\omega+3q+12}$ {ω + 0.2q} $GML_3^{15\omega+3q+12}$ {ω + 0.2q} $GML_6^{30\omega+6q+24}$ $GML_5^{5\omega+q}$		link-4
BIV.	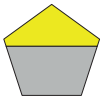	$SS_{1,3}$ $b_3^1 + b_3^2 > A$ b_3^1 & $b_3^2 > 0.5A$	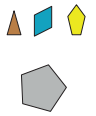	$GML_3^{15\omega+3q+12}$ {ω + 0.2q} $GML_4^{20\omega+4q+16}$ {ω + 0.2q} $GML_5^{25\omega+5q+20}$ {ω + 0.2q} $GML_5^{5\omega+q}$		link-4
C.		$SS_{1,3,C}$		$GML_3^{15\omega+3q+12}$ {ω + 0.2q} $GML_4^{20\omega+4q+16}$ {ω + 0.2q}		link-2
D.	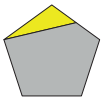	$VS_{1,2}$	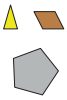	$GML_3^{15\omega+3q+12}$ {ω + 0.2q} $GML_5^{20\omega+4q+16}$ {ω + 0.2q} $GML_5^{5\omega+q}$	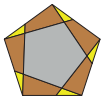	link-3
E.		$VS_{1,3}$		$GML_3^{15\omega+3q+12}$ {ω + 0.2q} $GML_3^{15\omega+3q+12}$ {ω + 0.2q} $GML_5^{25\omega+5q+20}$ {ω + 0.2q} $GML_5^{5\omega+q}$	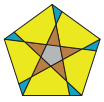	link-4
F.		$VS_{1,3,C}$		$GML_3^{15\omega+3q+12}$ {ω + 0.2q} $GML_3^{15\omega+3q+12}$ {ω + 0.2q}		link-2
G.		$VV_{1,3}$		$GML_3^{15\omega+3q+12}$ {ω + 0.2q} $GML_3^{15\omega+3q+12}$ {ω + 0.2q} $GML_5^{5\omega+q}$		link-3

Figure 6: Cutting of GML_5^n body with $n = 5 \cdot \omega + q$, with ω=0,1,2,… and q = 1,2,3,4,

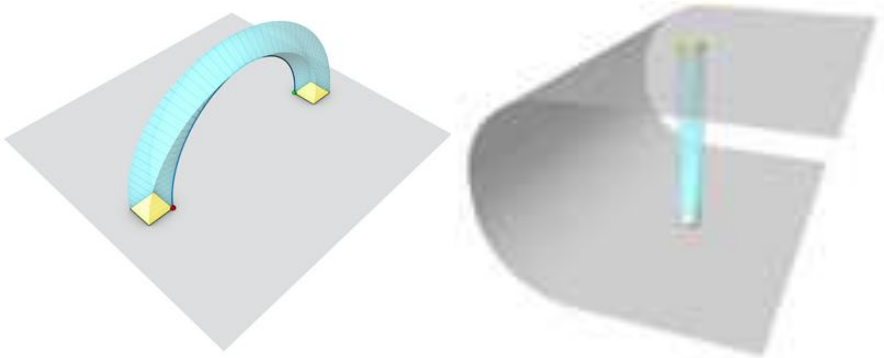

a **b**

Figure 7: GML_4^n structure connected via plane or brane cut [15]

If the twists are multiples of 180° however (i.e. $GML_4^{4\omega+2}$), then under certain conditions a Link-1 object results, namely in the case where the knife cuts through the center, which is always the case in a $VV_{1,3}$ cut (Case D in Figure 8b), and can also be the case for a $SS_{1,3}$ cut through the center (Case B.II in Figure 8b). In these two cases not only do we have a Link-1 body (quadrangular in cross section in Case B.II; triangular in cross section in case D), but they are also one-sided, and this is called the Möbius phenomenon, in analogy with the classic Möbius band.

In the process of cutting one can consider either a moving knife cutting a fixed GML_m^n body, or, alternatively, a moving (rotating) body and a fixed knife. Such a fixed knife can for example be fixed in the plane of Figure 7a and the GML_4^n body then moves, through the knife. Further, the knife may be a knife with a single blade or a multibladed knife. A moving knife with a single blade (Figure 8, case B.II) has to complete four periods to arrive again at its initial position, or the GML_4^n body has to complete four periods of rotation. If the knife has two perpendicular blades, one period suffices to cut the whole structure.

If the body is not twisted (Figure 8a), then cutting always results in two bodies. Similar considerations apply to GML_5^n, with all possible cuts for $n = 5 \cdot \omega + q$ in Figure 6. For cutting of hexagons all results have been classified in *[19]*.

Shapes of radial cross sections $GML_4^{4\omega}$	Cut	Parameters of the objects which appear after cutting			
		Shapes of radial cross sections	Structure of elements	Link group of elements	Link group of object
A.	$SS_{1,2}$		$GML_5^{5\omega}$ $GML_3^{3\omega}\{\omega\}$	Link-1	Link-2
B. a.	$SS_{1,3}$		$GML_4^{4\omega}$ $GML_4^{4\omega}\{\omega\}$		
B. b.	$S_{1,3,C}$		$GML_4^{4\omega}\{\omega\}$ $GML_4^{4\omega}\{\omega\}$		
C.	$VS_{1,2}$		$GML_4^{4\omega}$ $GML_3^{3\omega}\{\omega\}$	$\{0_1\}$	$\{(2\omega)_1^2\}$
D.	$VV_{1,3}$		$GML_3^{3\omega}\{\omega\}$ $GML_3^{3\omega}\{\omega\}$		

Shapes of radial cross sections $GML_4^{4\omega+2}$	Cut	Parameters of the objects which appear after cutting		
		Shapes of radial cross sections	Structure of elements	Link group of object
A.	$SS_{1,2}$		$GML_6^{6\omega+3}$ $GML_3^{6\omega+6}\{\omega+0.5\}$	Link-2
B.I	$SS_{1,3}$		$GML_4^{4\omega+2}$ $GML_4^{8\omega+8}\{\omega+0.5\}$	Link-2
B.II	$SS_{1,3,C}$		$GML_4^{8\omega+8}\{\omega+0.5\}$	Link-1
C.	$VS_{1,2}$		$GML_4^{4\omega+2}$ $GML_3^{6\omega+6}\{\omega+0.5\}$	Link-2
D.	$VV_{1,3}$		$GML_3^{6\omega+6}\{\omega+0.5\}$	Link-1

Figure 8 **a.** $GML_4^{4\omega}$; **b.** $GML_4^{4\omega+2}$ *[15]*

The Flatland Experience

Fortunately, the general solution for cutting GML_m^n with one or more knives has been found recently, by reducing the problem to planar geometry *[15, 20]*. The solution of the problem by a reduction of dimensions is reflected directly in the reduction of parameters in the analytic expressions.

To better understand cutting with a fixed knife, we can try to visualize what an inhabitant of Flatland would experience. In the 19th century, the mathematician Erwin A. Abbott wrote a story to explain to a large audience how one might think of a fourth dimension, by imagining a people consisting of circles or regular polygons [*21*]. They are clearly planar beings, living and thriving on their world-plane, but they are not able to experience a third dimension at all. When a sphere moves through Flatland all its inhabitants can observe is a circle of increasing and then of diminishing size, starting and ending with a point. Shock and awe.

Now, what does an inhabitant of Flatland observe when operations with 3D GML_m^n bodies or surfaces are carried out, in other words, when GML_m^n bodies rotate through Flatland? Or, when GML_m^n bodies do not rotate but the knives are moving? Or when we position the fixed knife in Flatland with rotating GML_m^n bodies? Shock and awe, once more.

At some instance in time an inhabitant of Flatland may find on h_{is}^{er} desk a hexagonal piece of paper with one knife across the paper (*VV, VS* or *SS* direction). The Flatlander has no idea how it got there but leaves it as it is. The next morning the Flatlander may see that the whole situation is still the same. However, it might also be that the "hexagonal piece of paper", which is actually a planar section of a GML_6^n, rotating through Flatland, is sliced into different zones; how many zones depends on the number of twists of the GML_6^n and the number of rotations through Flatland *[16]*.

Instead of a single knife there may also be multiple knives (Figure 9). The figures to the right in Figure 9 give the orientation of the knives for rotations of 60° due to torsion of GML_6^n, whereby the point of the arrow traces out a toroidal line.

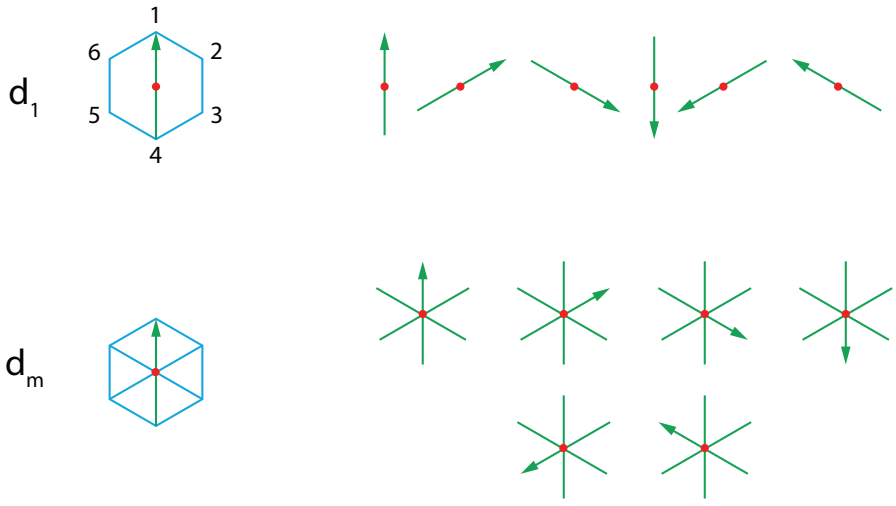

Figure 9: Cutting a hexagon with one-bladed d_1, or six-bladed $d_{m=6}$ knives.

Figure 10 gives all possible cuts with a one-bladed (d_1, upper row) and six-bladed knife (d_6, lower row) for GML_6^n bodies. The six-bladed knife consists of six copies of the one-bladed knife by rotation over 60° (but they overlap two by two giving the appearance of three blades).

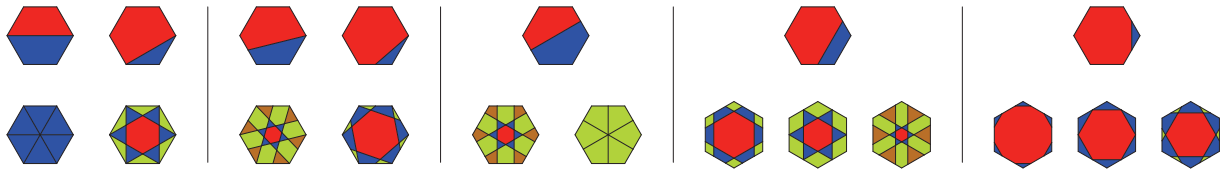

Figure 10: All possible cuts with one-bladed d_1, or six-bladed $d_{m=6}$ knives

If the GML_m^n structure cuts through Flatland as the square GML_4^n body in Figure 7a, someone else in Flatland can observe a second, identical phenomenon. If both Flatlanders come into contact with each other, they will find that one square is somehow turned by 90°. In Euclidean geometry, one cannot distinguish between two squares rotated by 90° or a multiple thereof. If the GML_m^n bodies are twisted, experimental identification of differences may be performed on the ground. In one case the diagonal runs "North to South", in the other one "East to West".

Without knowing the GML_m^n structure and number of knives, Flatlanders are bamboozled by this spooky action at a distance. If the Flatlanders try to untangle the mystery, by repeating or experimentally using other knives and positions, this will result in fully predictable structures, and reproducible phenomena elsewhere in Flatland. Only when one brave Flatland soul travels into the third dimension it will be revealed what actually happens. And like in the original story, upon returning the brave soul will have a hard time convincing his co-planar Flatlanders.

The Möbius phenomenon for GML with polygonal cross section

The conditions for Möbius phenomenon

Our main motivation is the search for conditions under which the complex structure remains a single surface or body. This reduces complexity, especially if GML surfaces and bodies represent physical phenomena. When a classic Möbius band is cut along the center of the band, one obtains a single (Link-1) surface, which is single-sided, like the original band *[1]*. This is known as the Möbius phenomenon. Cutting through the center is crucial. Extending this to GML_m^n bodies, it was observed that this Möbius phenomenon, whereby the cutting process yields only a single and "one-sided" body, occurs only for cross sections of polygons with an even number of vertices and sides and only in the specific case when the knife cuts through the center of the polygon. In Figure 8a the results of cutting $GML_4^{4\omega}$ are shown where $\omega = 0,1,2$ .... This conforms to no twists (for $\omega = 0$) or twists of 360° (for $\omega = 1,2,...$). The link group of the object is always Link-2, and no single body can be obtained.

If on the other hand, the twists are multiples of 180° (i.e., $GML_4^{4\omega+2}$), then under certain conditions, a Link-1 object results, namely in the case where the knife cuts through the center. This is always the case in a $VV_{1,3}$ cut (Case D in Figure 8b) and for a $SS_{1,3}$ cut through the center (Case B.II in Figure 8b). In these two cases not only do we have a Link-1 body (quadrangular in cross section in Case B.II; triangular in cross section in case D), but they also display the Möbius phenomenon. On the other hand, in Figure 6 one observes that a Link-1 phenomenon does not occur for a pentagonal cross section *[4]*.

The conditions to obtain Link-1 objects with the Möbius phenomenon are *[22]*:

1. a cut through the center, and
2. the rotational symmetry of the cross section m has to be an even positive integer.

The Möbius phenomenon is never observed if m is odd, for this specific way of cutting.

One additional observation, going beyond regular polygons, was that these conditions also lead to the fact that at the connection point the cross sections have to ensure a smooth transition, a condition which is met when the two sides are congruent when rotated around the center (corresponding to the original Möbius band of Figure 1a). In Figure 11 these conditions are met for cases **a.** and **b.** but not for **c.** This observation led to extending the possibility to obtain a Link-1 structure after cutting, to odd polygons.

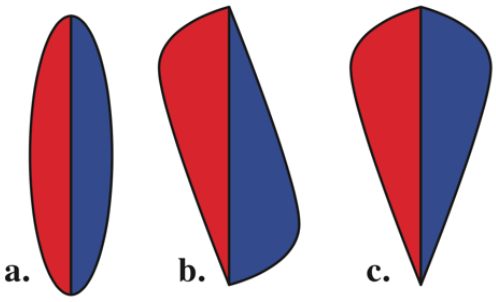

Figure 11: Two angular bodies with cut through the center.

The Möbius phenomenon for m=even and m=odd polygons

In all foregoing cases knives are defined to cut the whole cross section or, in other words, cutting the boundary at two points. Such knives are called chordal knives, in analogy with chords cutting a circle (leading to classical definitions of the trigonometric functions). The analytical definition is given in *[16, 20].*

When taking into account the conditions of congruence and rotational symmetry (Fig. 11a and b), it was found that the Link-1 and Möbius phenomenon could also be extended to odd polygons, by the use of **radial** knives *[13, 22].*

Definition 7: Radial knives are knives that cut the boundary only in one point. Hence the origin of the knife is contained within the boundary of the cross section and can be the center.

In Figure 12 one-bladed chordal and radial knives are shown (with the special case of the radial knife originating in the center of the polygon). This also has consequences for how many blades a knife has. The six-bladed $d_{m=6}$ knives in Figure 9 can be considered either as a six bladed radial knife with each blade originating in the center and cutting the boundary only once, or as a six-bladed chordal knife cutting the boundary twice.

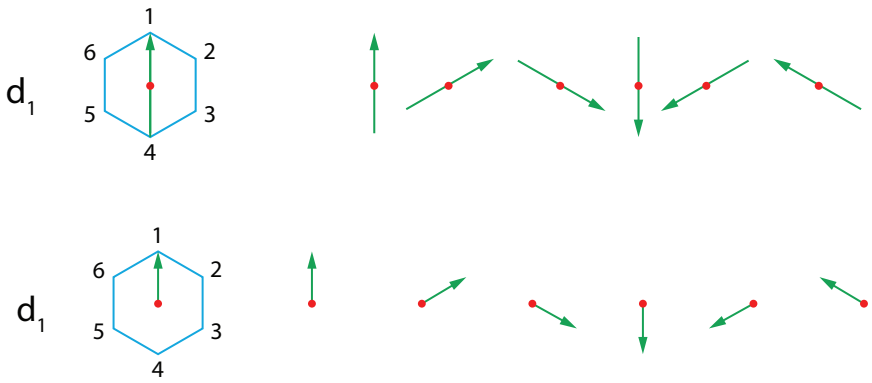

Figure 12: Chordal and radial one-bladed d_1 knives

In the case of $m =$ odd regular polygons however, it is precisely the use of chordal knives, which prevents the occurrence of Link-1 bodies. This is easily seen as follows: In the case of m radial knives, the number of sectors after cutting is m, irrespective whether m is even or odd. In Figure 13 results from the cutting of equiangular triangles are shown; the cut is either with chordal knives through the origin from vertex to side (Figure 13a), or from side to side (Figure 13c). Three chordal knives result in $2m = 6$ sectors. These sectors are a combination of one light blue and one dark blue sector in Figure 13a and c. The sectors are congruent, but only two by two rotationally symmetric. Dark and light blue adjacent sectors are congruent but are mirror images. Hence, they do not satisfy the condition of rotational symmetry.

Figure 13: Vertex to side and side to side cuts through the origin in a triangle, with chordal (a and c) or radial knives (b and d) *[13]*.

The use of radial knives with origin in the center on the other hand, leads to three $(m = 3)$ sectors which are both congruent (Figure 13 b and d) and rotationally symmetric around the origin. In the 3D GML_3^n bodies with $m = n$ twists, this results in one body after cutting, with Möbius phenomenon, but now also for odd polygons.

Hence, we have the following theorem [13]*: "If the knife cutting a GML_n^n body is a radial knife with its origin in the center of the polygonal cross sections and cuts all sides of the polygon with equal spacing, the Möbius phenomenon will occur in both odd and even polygons".*

From these conditions it is clear that the knife does not have to be a straight one; nor does the cross section have to be a regular polygon, as long as rotational symmetry is conserved, and the conditions of cutting are met. Furthermore, Equations (1) and (2) allow for a kinematic and dynamic study of GML_n^n bodies with a time t parameter, but the study of cutting was shown to be reduced to:

- the shape of the cross section, defined by m, and
- the number of twists defined by n.

A major question then arose on the effect or importance of any change in cross sections along the GML_n^n body, deviating from the rotational symmetry. The answer is the major result of this paper.

One section is a sufficient condition

In all previous works it was tacitly assumed that the cross section of the GML_m^n remains constant along the whole structure, whereas the equations (1) and (2) allow for a changing cross section along the GML_m^n. In Figure 11 examples of two-angular cross sections were given which do (11a and b) or do not (11c) meet the conditions. A direct example of a GML_m^n body with changing cross section is when the cross sections change along the body, for example in sequences *a-b-c-a*, or *a-b-c-b-a*. The changes can occur smoothly or in discrete jumps.

The question then is whether all cross sections have to retain the condition of rotational symmetry, to achieve the Link-1 or Möbius phenomenon. For example, will a Link-1 structure still occurs if the cross sections of the GML_m^n change from the starting point, where the conditions are met, to an intermediate section that does not meet these conditions, and again closing with the original cross section? The answer is:

***Theorem 1**: In the cutting of GML_m^n bodies under the above conditions (radial knife cutting through the center for both odd and even regular polygons, or chordal knife cutting through the center for even regular polygons) a sufficient condition is that only one cross section is rotationally symmetric, to obtain the Link-1 result with the Möbius phenomenon.*

Proof: The cross sections at the start and end of the GML_m^n body are the same. If cross sections are denoted as $S_0, S_1, S_2, \dots, S_q$, then the set of all cross sections is denoted as $[S_0, S_1, S_2, \dots, S_q]$. The sequence of cross sections is continuous for $q \to \infty$ and discrete (or at least partially discrete, partially continous) for $q < \infty$. The condition for a smooth joint of both ends is when $S_0 = S_q$. Additionally the orientation of both is twisted before joining (e.g. 180° in the case of a square), denoted as $\uparrow S_0 = \downarrow S_q$.

For cutting, one can assume the same, constant shape along the whole GML_m^n bodies, so that the knife follows the classical toroidal lines (ribs or slit surfaces) (e.g,. Figure 5a). In this case only S_0 and S_q are relevant, but not $]S_1, S_2, \dots, S_{q-1}[$, and the cutting then reduces to the general case of cutting GML_m^n bodies [1,16] ■

Equations (1) and (2) include a time variable t, important if the GML_m^n body represents any physical or biological system. For the proof of Theorem 1 a simplified version can be used, since only the cross section $p(\tau, \psi)$ and the twisting parameter n, are involved.

Some consequences

The above result is remarkable, since one can always find a way of cutting (or division of zones) whereby at the end of the day, the whole shape turns out to be a one-sided body, coherent in any sense of the word. As long as one cross section fulfills the conditions, all other cross sections $]S_1, S_2, \dots, S_{q-1}[$ may be anything. Going back to Figure 4: if only one cross section is the cross section of Figure 4a (or case B.III and B.IV in Figure 6b), all other cross sections may be dispersed data points as in Figures 4b,c,d. As long as the cut is executed in the correct way (i.e., a chordal knife through the center for even polygons, or a radial knife originating in the center for even and odd polygons) it follows that the structure is a one-sided Link-1. In case the cross sections are larger or outside the boundaries of the start and end, one simply can use knives with longer blades. We will give four illustrative examples.

Example 1 with maximum entropy: Consider a *GML* body with hexagonal cross section as shown in Figure 14. This example was actually used to illustrate twisted fibre bundles in [23]. Since the Möbius band is the simplest non-trivial example of a fibre bundle, this also shows the generality of our results. We consider one cross section of Figure 14a. Here, the GML_6^n has constant cross section and according to Theorem 1 it suffices that only one cross section is a hexagon. All other cross sections may morph into pentagons, starfish, superellipses or any shape imaginable. The cross sections may even become a point as in a double cone. Or the cross section can be a point, so that the GML structure is a line, except for the sections S_0 and S_q. Further, the cross sections may consist of dispersed data points, distributed according to some probability (density) function or randomly (maximum entropy). As long as the cut is executed correctly, the result will be a single body (Link-1), displaying the Möbius phenomenon of one-sidedness.

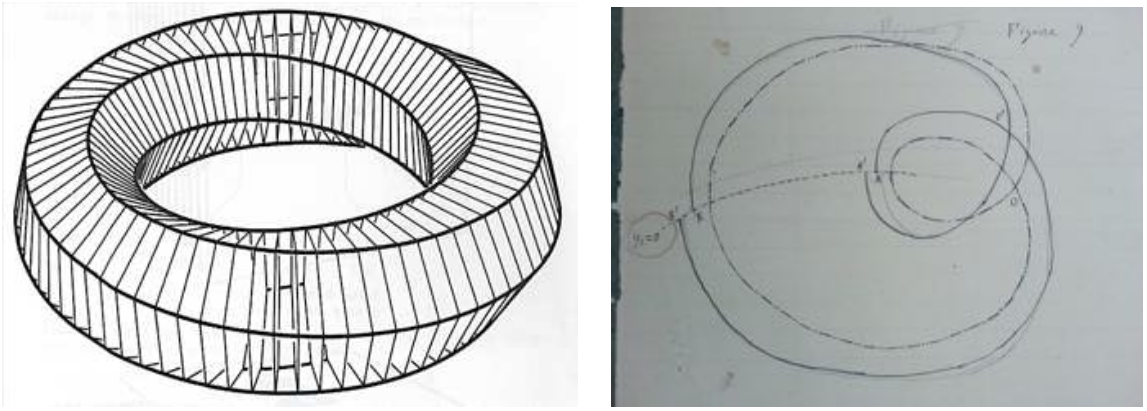

a **b**

Figure 14a: Fiber bundle [23], b. Poincaré's original figure [24]

Example 2 with redundancy: Consider a chess board with a knight moving across the board. It is then possible for the knight to touch every square exactly once; the tour is closed if the knight arrives back at the original square. A closed tour of the knight corresponds to the condition $S_0 = S_q$. For an 8x8 chess board there are trillions of possible closed tours [25;26]. Hence, if $S_1, S_2, \dots, S_{q-1}$ represent the different sequences of the squares on a chess board for one closed knights tour, there are many ways of arranging the sections $]S_1, S_2, \dots, S_{q-1}[$, with S_1, S_{q-1} one knight's move away from $S_0 = S_q$. But if the conditions of cutting are met, then neither of the sections $S_1, S_2, \dots, S_{q-1}$, nor their arrangement play any role; the result of cutting will be a single Link-1 body.

Example 3 with area conservation: Arnold's Cat. In many physical and mathematical cases conservation of area (or volume) is crucial. In Figure 14a, all sections have the same area, but what the hexagons contain can be very different. One example with area (or volume) conservation is Poincaré's Recurrence Theorem, which states that any dynamical system will return arbitrarily close to its initial state after a certain time (Figure 14b). More precisely, Poincaré proved that in certain systems almost all trajectories return arbitrarily close to their initial position infinitely often. If a flow preserves volume and has only bounded orbits, then for each open set there exist orbits that intersect the set infinitely often.

Arnold's Cat is the most famous illustration of the phenomenon [27; 28]. Starting with the image of a cat, and performing an area preserving transformation eventually, after a specific number of discrete steps, the image of the cat completely reappears, and will continue to do so, infinitely. The transformation tears up the image, but maps it back to fit the original square in every step, hence it is area-preserving (one can imagine that each section in Figure 14a except one, has the same hexagon as boundary, but the domains inside may look random or disordered). In [28] plant leaves defined by Gielis curves were subjected to such Anosov transformation to illustrate the Poincaré Recurrence phenomenon.
Obviously, in a GML body the cat or the leaves may be one cross section (beginning and end) and all other cross section can be the intermediate discrete steps and are of the same area as the initial one, since the transformation is area-preserving. If the image has rotational symmetry, one can cut the GML body through the center and the result will be a single, one-sided body.

Example 4: Flatland revisited. Figure 7b shows a GML_4^n structure connected to a brane, illustrative of wormholes. Since the two sections at the brane are the same, namely S_0 and S_q, one can define the cutting process

in such a way that, whatever goes in comes out the same on the other side, so that everything remains connected as a Link-1 irrespective of what happens inside the wormhole. A final conclusion is that the young Flatlander in Abbot's story must have been extremely lucky to observe the full sphere. Those who stayed behind would have witnessed growing and waning circles, whereas in 3D everything might have been dust.

The set of examples can be extended without bounds.

References

1. Tavkhelidze IN. About connection of the generalized Mobius- Listing's surfaces with sets of ribbon knots and links. In: Proceedings of Ukrainian Mathematical Congress, S.2 Topology and Geometry, vol. 2, 2011, pp. 177–190. ISBN 978-966-6193-8, Kiev, Ukraine
2. Starostin, E. L., & Van Der Heijden, G. H. M. (2007). The shape of a Möbius strip. Nature Materials, 6(8), 563-567.
3. Tavkhelidze, I. On the some properties of one class of geometrical figures and lines, Reports of Enlarged Sessions of the Seminar of I. Vekua Institute of Applied Mathematics, vol. 16, N. 1, 35–38 (2001), Tbilisi, Georgia.
4. Ricci, P. E., & Tavkhelidze, I. (2011). About some geometric characteristics of the generalized Möbius–Listing surfaces. Georgian Mathematical Journal, 18(2), 329-343.
5. Tavkhelidze, I., Gielis, J., & Pinelas, S. (2020). About Some Methods of Analytic Representation and Classification of a Wide Set of Geometric Figures with "Complex" Configuration. In International Conference on Differential & Difference Equations and Applications (pp. 347-359). Springer, Cham.
6. Tavkhelidze, I., Caratelli, D., Gielis, J., Ricci, P.E., Rogava, M., Transirico, M.: On a geometric model of bodies with "Complex" configuration and some movements. In: Modeling in Mathematics, pp. 129–158. Atlantis Press, Paris (2017)
7. Chubelaschwili, D., Pinkall, U. Elastic strips. Manuscripta Math. 133, 307–326 (2010). https://doi.org/10.1007/s00229-010-0369-x
8. Nishiguchi, N., & Wybourne, M. N. (2018). Phonon modes in a Möbius band. Journal of Physics Communications, 2(8), 085002.
9. Herges, R. (2006). Topology in chemistry: designing Möbius molecules. Chemical Reviews, 106(12), 4820-4842.
10. Schaller, G. R., & Herges, R. (2013). Möbius molecules with twists and writhes. Chemical Communications, 49(13), 1254-1260.
11. Schaller, G. R., Topić, F., Rissanen, K., Okamoto, Y., Shen, J., & Herges, R. (2014). Design and synthesis of the first triply twisted Möbius annulene. Nature Chemistry, 6(7), 608-613.
12. Caetano, E. W., Freire, V. N., Dos Santos, S. G., Galvao, D. S., & Sato, F. (2008). Möbius and twisted graphene nanoribbons: Stability, geometry, and electronic properties. The Journal of Chemical Physics, 128(16), 164719.
13. Gielis J., Tavkhelidze I. (2021) The Möbius phenomenon in Generalized Möbius-Listing bodies with cross section of odd and even polygons. Growth and Form (in the press)
14. Zaslavsky, G.M., Sagdeev R.Z., Usikov, D.A., Chernikov A.A. (1991) Weak Chaos and quasi-regular patterns. Cambridge University Press, Cambridge.
15. Tavkhelidze, I., & Ricci, P. E. (2017). Some Properties of "Bulky" Links, Generated by Generalised Möbius–Listing's Bodies GML_m^n. In Modeling in Mathematics (pp. 159-185). Atlantis Press, Paris
16. Gielis, J., & Tavkhelidze, I. (2020). The general case of cutting of Generalized Möbius-Listing surfaces and bodies. 4open, 3, 7. https://doi.org/10.1051/fopen/2020007
17. Huang, W., Li, Y., Niklas, K. J., Gielis, J., Ding, Y., Cao, L., & Shi, P. (2020). A Superellipse with Deformation and Its Application in Describing the Cross-Sectional Shapes of a Square Bamboo. Symmetry, 12(12), 2073.
18. Shi, P. J., Huang, J. G., Hui, C., Grissino-Mayer, H. D., Tardif, J. C., Zhai, L. H., ... & Li, B. L. (2015). Capturing spiral radial growth of conifers using the superellipse to model tree-ring geometric shape. Frontiers in Plant Science, 6, 856.
19. Pinelas, S., & Tavkhelidze, I. (2017). Analytic Representation of Generalized Möbius-Listing's Bodies and Classification of Links Appearing After Their Cut. In International Conference on Differential & Difference Equations and Applications (pp. 477-493). Springer, Cham.
20. Tavkhelidze, I., & Gielis, J. The process of cutting GML_n^m bodies with d_m-knives. In Reports of the Enlarged Sessions of the Seminar of I. Vekua Institute of Applied Mathematics, Vol. 32, 2018.

21. Abbott, E.A., Flatland, A Romance of Many Dimensions. By A. Square. Seeley, London (1884)
22. Gielis J., Tavkhelidze I. The Möbius phenomenon in Generalized Möbius-Listing bodies with cross section of odd and even polygons. Report of the Enlarged Sessions of the Seminar of I. Vekua Institute of Applied Mathematics volume 34, 2020.
23. Weeks, J. R. The Shape of Space. How to Visualize Surfaces and Three-dimensional Manifolds. Marcel Dekker. Chapter 17 Bundles (1985)
24. Poincaré, H. (1890) Sur le problème des trois corps et les équations de la dynamique. Acta Math. 13: 1–270.
25. Gardner, M. "Knights of the Square Table." Ch. 14 in Mathematical Magic Show: More Puzzles, Games, Diversions, Illusions and Other Mathematical Sleight-of-Mind from Scientific American. New York: Vintage, pp. 188-202, 1978.
26. Weisstein E.W Knight Graph. From Mathworld -A Wolfram Web Resource.
27. Weisstein E.W Arnold's Cat Map. From MathWorld--A Wolfram Web Resource.
28. Mishra, S. K. (2014). A note on Poincaré recurrence in Anosov diffeomorphic transformation of discretized outline of some plant leaves. Available at SSRN 2472318.